Finite Element Analysis by Mesh Refinement of Isotropic Rectangular Plate with Centred and Off-Centred Hole

Greg Kurzepa

March 2024

Note to marker: Since I did not do the 3D7 lab, I've included its results in this FTR report. Every section is split into analysis of the symmetric plate and asymmetric plate. To read what is relevant for the FTR only, skip over the symmetric plate bits.

1 Summary

Finite Element (FE) analysis is a ubiquitous and essential tool in modern engineering, allowing complex physical differential equations to be approximately solved over arbitrary domains to arbitrary accuracy, given sufficient boundary conditions. An example is the analysis of stresses and displacements in a material given loading. Here, stresses and displacements in a 2D isotropic steel plate with a hole loaded horizontally on its edges were found using FE analysis. The accuracy and convergence speed on a relevant plastic failure metric were assessed with regards to various shape functions and mesh refinements. It is shown in this case that denser meshes, quadratic (over linear) shape functions, and selective element size distributions can increase accuracy. Adaptive mesh refinement is suggested as a further improvement.

2 Method

2.1 Reproduction

The code, results and data can be found at
`https://github.com/suspicious-salmon/CUED-3D7-Lab-main`

2.2 Physical Problem and Boundary Conditions

2.2.1 Symmetric Plate

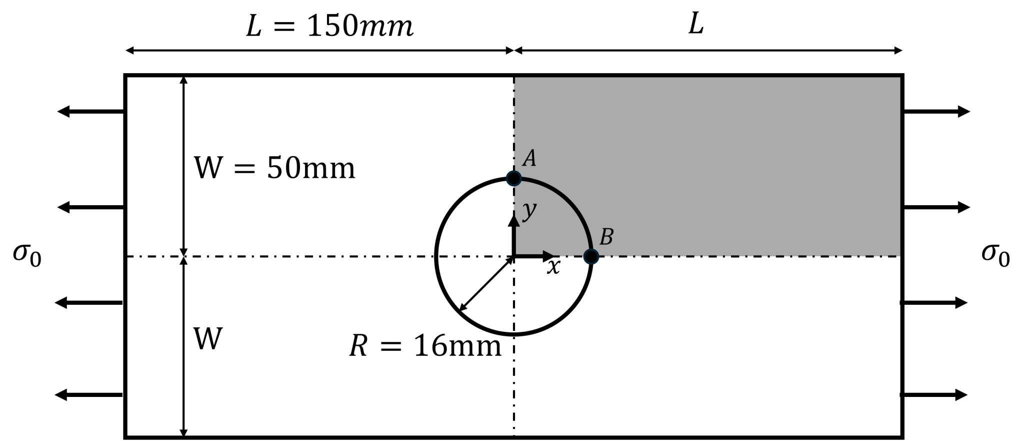

Figure 1: Geometry of the symmetric plate used in the FE model. The greyed area is the area that was used for the mesh in the simulation.

The rectangular plate (fig. 1) with a centred hole has 2 axes of symmetry; one along the x-axis and one along the y-axis with the origin at the hole's centre. Thus only one quadrant is necessary for the full solution (here the upper-right corner was used).

Dirichlet displacement $\mathbf{u}(x, y)$ boundary conditions were set to maintain this symmetry - the displacement of the plate perpendicular to the symmetry axes was set to zero:

$$u_x(x = 0) = 0 \tag{1}$$

$$u_y(y = 0) = 0 \tag{2}$$

The force boundary condition was set such that

$$\sigma_{xx}(x = L) = \sigma_0 \tag{3}$$

and zero otherwise.

2.2.2 Asymmetric Plate

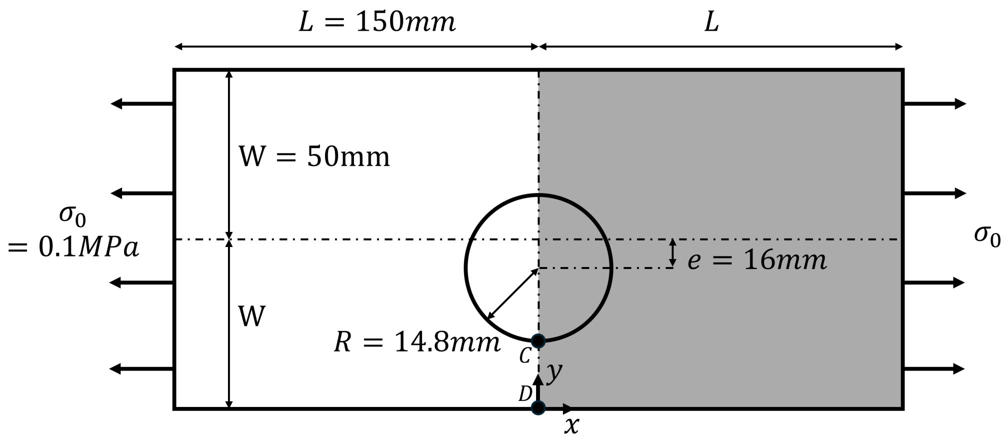

Figure 2: Geometry of the asymmetric plate used in the FE model. The greyed area is the area that was used for the mesh in the simulation. The coordinate system keeps the greyed area within the +ve quadrant - I ran into errors when trying to solve a system with nodes in other quadrants.

The rectangular plate (fig. 2) with the hole vertically off-centre by distance e has 1 axis of symmetry along the y-axis. One half of the plate is necessary to find the full solution (the right half of the plate was used).

Dirichlet displacement $\mathbf{u}(x, y)$ boundary conditions were set such that displacement of the plate perpendicular to the symmetry axis was zero. Additionally, the vertical displacement of one node on the hole boundary was set to zero to prevent the deformed mesh from moving unpredictably in that axis.

$$u_x(x = 0) = 0 \tag{4}$$

$$u_y(x = r, y = 0) = 0 \tag{5}$$

The force boundary condition was again set such that

$$\sigma_{xx}(x = L) = \sigma_0 \tag{6}$$

and zero otherwise.

The plate was also analysed by applying a uniform displacement along the right end instead of a force. Applying displacement boundary conditions instead of forces is a way to reduce problem instability.

$$u_x(x = L) = u_0$$

2.3 Meshes and Shape Functions

2.3.1 Symmetric Plate

To assess the impact of mesh design, the analysis was run with linear shape function for 3 different meshes l1, l2, l3 (fig. 3). To assess the impact of shape function choice, mesh q1 was analysed with both a linear and quadratic shape function.

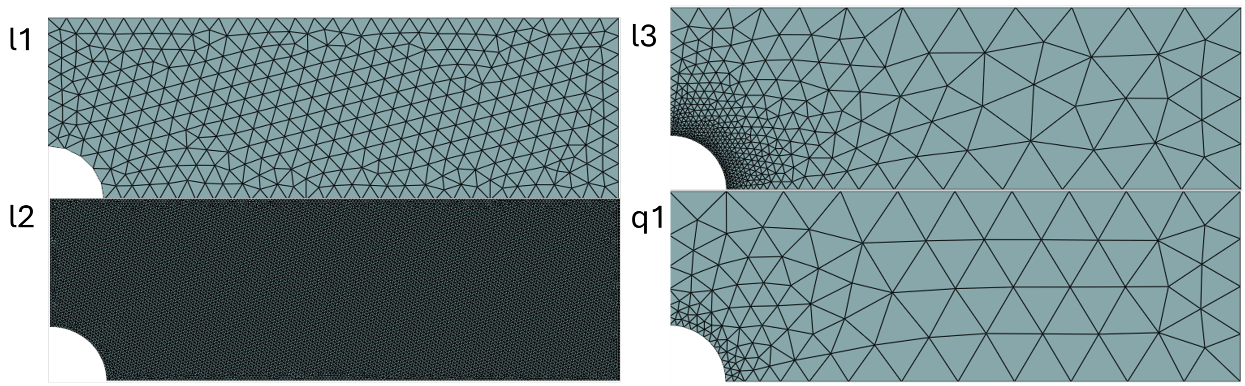

Figure 3: l1, l2 and l3 were used to test linear shape function only. q1 was used to test both a linear and quadratic shape function. **l1**) Mesh with uniform element size and 829 elements. **l2**) Uniform element size and 25937 elements. **l3**) Element size varies quadratically from origin (bottom-left of mesh). 987 elements. **q1**) Element size varies quadratically from origin. 259 elements.

2.3.2 Asymmetric Plate

For the case of loading with a uniform stress σ_0, I tested the convergence of 3 different mesh size distributions. Convergence was measured with respect to increasing number of elements and increasing computation time. The meshes all had quadratic shape function and had element size distributions which varied as a function of distance from the hole centre: logarithmically, quadratically and quartically (fig. 4). Each distribution was tested for approximately 500, 2000, 8000 and 16000 elements, and the average time taken for 3 finite element displacement solutions to be calculated was measured.

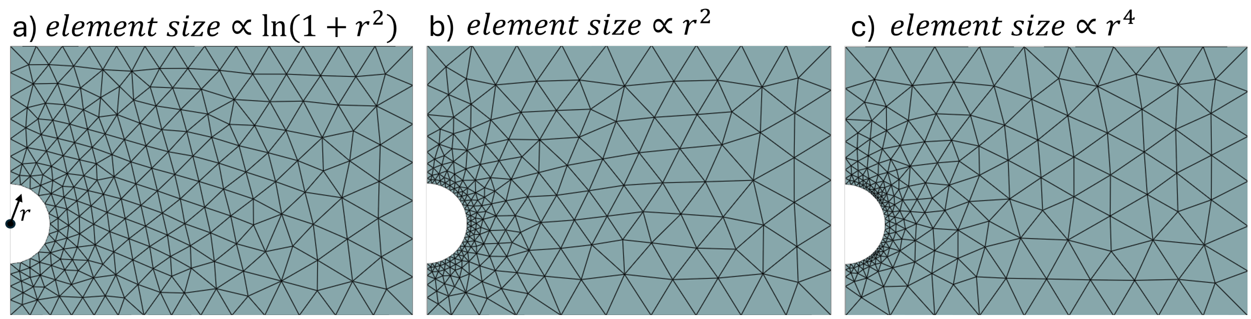

Figure 4: One mesh from the 3 different element size distributions used, each with approximately 500 elements. Each distribution a (logarithmic), b (quadratic), c (quartic) was also tested with approximately 2000, 8000 and 16 000 elements to assess convergence.

For the loading indirectly applied by uniform displacement u_0, a mesh with quadratic shape function, quadratically varying element size from hole centre and approximately 16 000 elements was used.

2.4 Evaluation

2.4.1 Metrics

For all experiments, the maximum Von Mises stress anywhere on the plate was predicted. In 2D, Von Mises stress σ_v is calculated from the local horizontal and vertical stresses yielded by the FE model using the 2nd invariant of deviatoric stress, J_2:

$$\sigma_v = \sqrt{3J_2} = \sqrt{\frac{1}{2}(\sigma_{xx} - \sigma_{yy})^2} \tag{7}$$

If the metal follows the Von Mises yield criterion, this measure describes how close a point on the plate is to yield. When the Von Mises stress at a point becomes equal to the yield stress, the metal yields at that point:

$$\sigma_v = Y \tag{8}$$

The maximum anywhere on the plate describes how close the overall plate is to yielding somewhere.

2.4.2 Symmetric Plate

To evaluate the accuracy of the analysis, the FE stress concentration factor at two points A and B on the edge of the hole (fig. 1) was compared to the theoretical value for a semi-infinite plate as calculated by Howland (Liu and Clarkson (2023)).

Additionally, the FE stress was compared to the exact theoretical solution along the x and y axes for an infinite plate loaded horizontally, and with a set of experimental results for σ_{xx} along the y-axis obtained from the 3C7 lab. I used the results provided for the 3D7 lab.

2.4.3 Asymmetric Plate

The convergence metric used was maximum Von Mises stress.

First, the simulation was run with the hole centred ($e = 0$) to verify that the results of the new geometry are still accurate.

Then, convergence of each mesh type was tracked to assess roughly the accuracy of the solution.

Additionally, the FE stress was compared to the theoretical solution calculated by Mindlin for a semi-infinite plate with one straight edge boundary close to the hole (Liu and Clarkson (2023)).

3 Results

3.1 Symmetric Plate

Mesh and Shape Function	Number of elements	Predicted σ_{xx}/σ_0 at A	Error to Howland	Predicted σ_{yy}/σ_0 at B	Error to Howland	Predicted Maximum Von Mises Stress (Mpa)
l1 linear	829	2.314	-31.0%	-0.399	68.2%	160.5
l2 linear	25937	3.029	-9.6%	-1.085	13.5%	176.1
l3 linear	987	3.094	-7.7%	-1.046	16.6%	175.1
q1 linear	259	2.545	-24.0%	-0.692	44.8%	164.3
q2 quadratic	259	3.262	-2.7%	-1.158	7.6%	179.2

Table 1: Selected metrics for each symmetric FE simulation. The Maximum Von Mises stress is the highest predicted Von Mises stress anywhere on the mesh. The Howland stress concentration factors were 3.351 at A and -1.254 at B. The remote stress σ_0 was 58MPa.

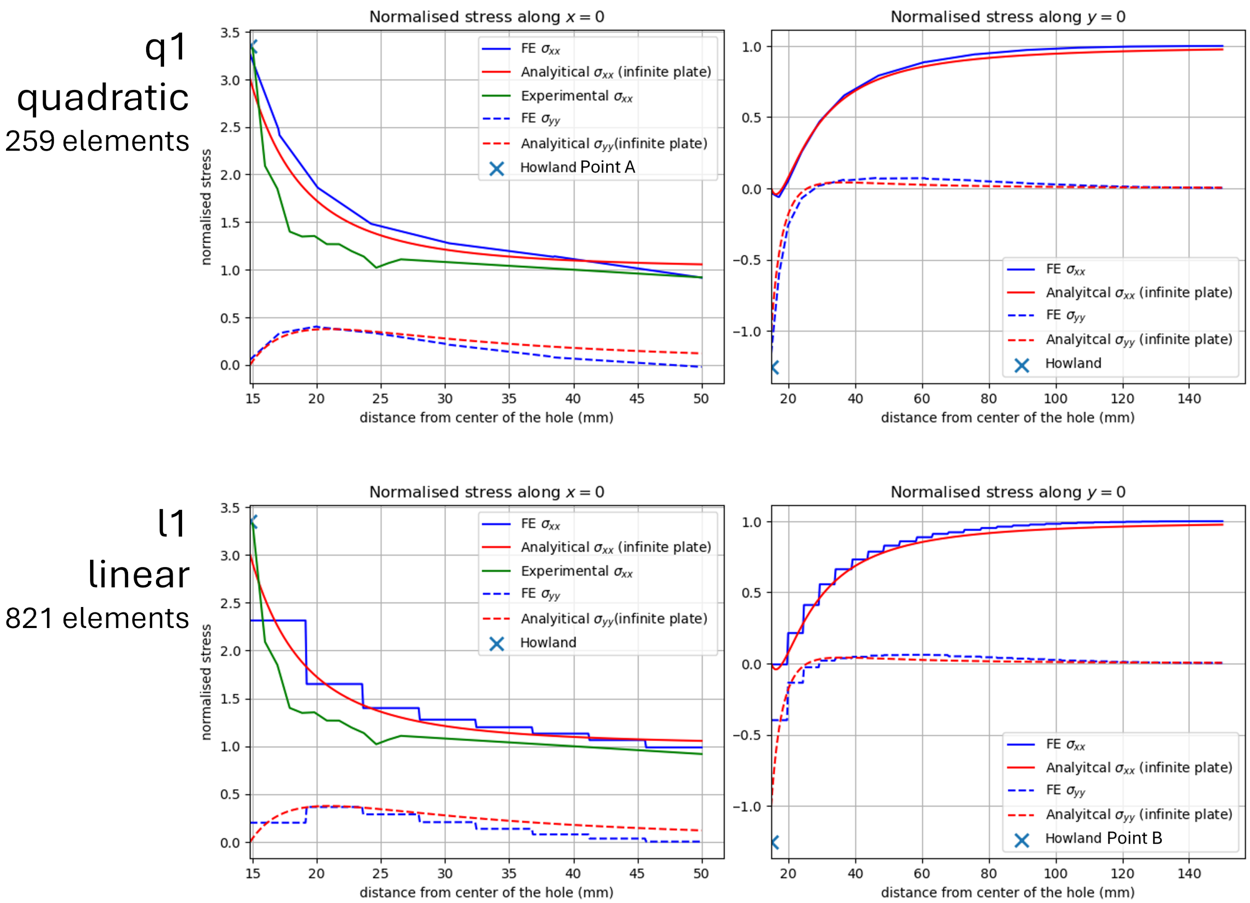

Figure 5: Calculated normal stress concentration factors along the x and y axis of the symmetric plate (blue) for l1 (which had the largest error compared to the Howland solution) and q1 with the quadratic shape function (which had the smallest). They are compared to theoretical infinite plate (red) and Howland (crosses) solutions, as well as a set of experimental measurements (green).

3.2 Asymmetric Plate

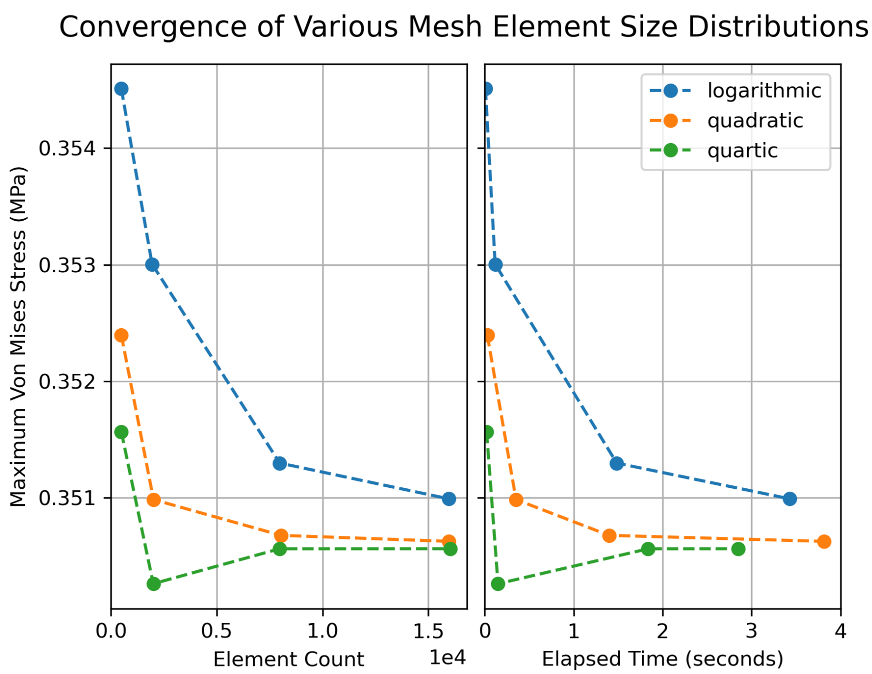

Figure 6: caption

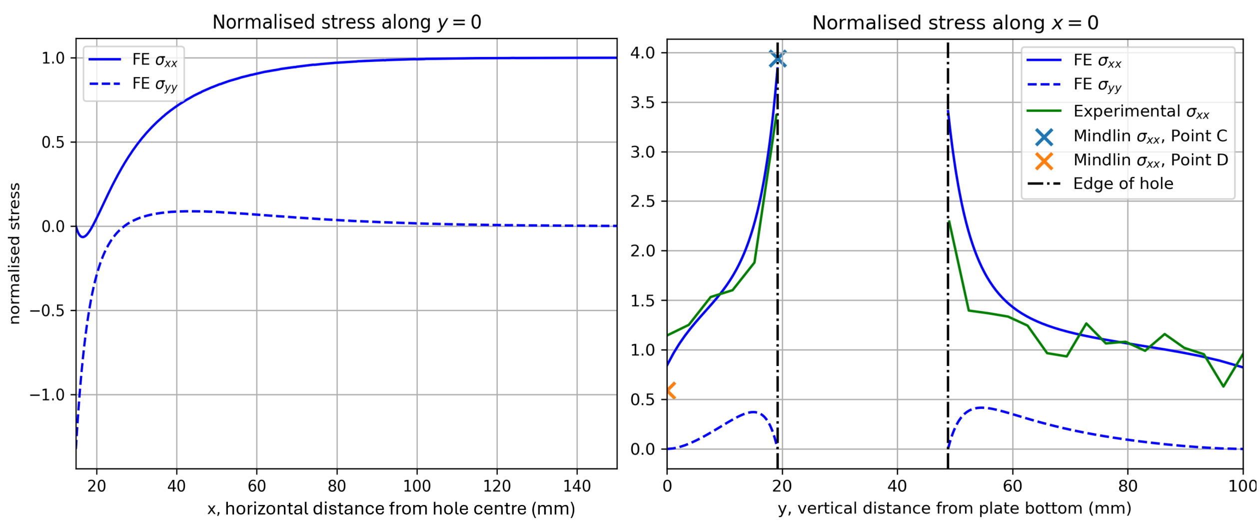

Figure 7: Stress profiles along x and y axes (as on the un-deformed plate) for the asymmetric quadratically-varying mesh with 16 000 elements.

Figure 8: Von Mises stress (as on the un-deformed plate) for the asymmetric quadratically-varying mesh with 16 000 elements. Units are in MPa.

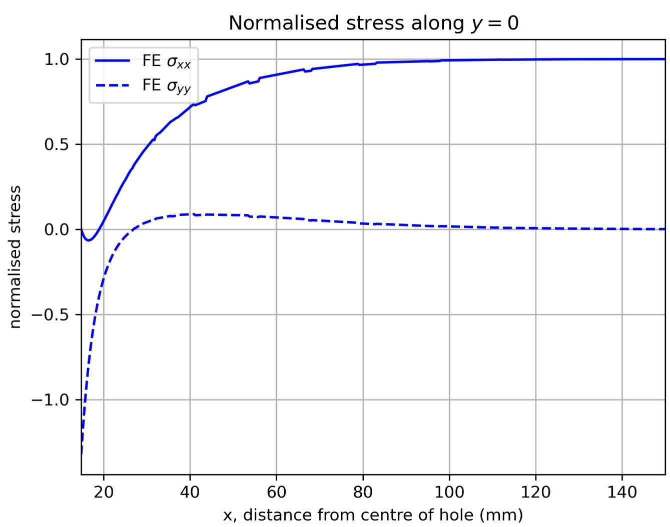

Figure 9: Stress profile along the x-axis for the asymmetric quartic plate with 16 000 elements. The solution seems to have some erratic fluctuations at the mid-distances.

4 Discussion

Generally, the FE model most struggled to accurately predict stress concentrations at the highly-stressed top edge of the hole. This could reflect a general need for greater mesh refinement in areas with large stress variations.

4.0.1 Symmetric Plate

The metrics in table 1 were chosen because:

- The comparison between predicted and Howland stress concentration factors evaluates the accuracy of each simulation. This is flawed, since the Howland solution assumes infinite plate length L, but stress decays to σ_0 quickly along the x-axis so the difference between Howland and the true value for this scenario should be small.
- An accurate prediction of maximum Von Mises stress is important in design: if it exceeds the yield stress of the material, the part will begin to yield at that point, which is usually undesirable.

table 1 suggests that:

- (l1 - l2) Meshes with more elements improve accuracy.
- (l2 - l3) Placing more elements in complicated areas with large stress variations improves accuracy.
- (q1 - q2) Using a quadratic instead of linear shape function improves accuracy, especially at boundaries and areas with large stress variations.

These simulations were run with $\sigma_0 = 58Mpa$. To verify that the FE results follow superposition, I ran the simulations again with $\sigma_0 = 10MPa$, and the results scaled proportionally to within 0.1% error. Using this as justification, I calculated that the expected remote stress to cause first yield in an equivalent Aluminium plate (yield strength $200Mpa$) is $66.25MPa$.

4.0.2 Asymmetric Plate

All 3 mesh types converged towards a similar prediction of maximum Von Mises stress (fig. 6). This suggests that the FE problem was well-conditioned and is providing realistic predictions. The quadratic and logarithmic meshes, with the small sample size used, converge monotonically (without back-and-forth fluctuation) so seem like more reliable meshes to use than the quartic mesh. The dataset, though, is small so (as is also true in the rest of this discussion) more rigorous tests might be needed when developing a finite element model in practice.

The mesh refinement here is very simple and is not optimal for this problem. The magnitude of stress variation in the plate does not just decrease as a function of the radius: fig. 8 shows that there is significant stress variation along the diagonals some distance from the radius that would benefit from fine elements. This could be the cause of the inaccuracy in the quartic mesh, which had the coarsest elements at those mid-distances. It is reflected in a slightly erratic mid-distance stress distribution along the x-axis (fig. 9), unlike the quadratic solution (fig. 7) and logarithmic solution.

The most reliable way to verify that the FE results are accurate would be to perform the experiment in real life, taking more accurate readings than the ones presented here. For this plate, some sanity checks can also be performed. For example, the width of the top part of the plate (above the hole) could be made very large, effectively making the simulation equivalent and thus comparable to the Mindlin result that was plotted in fig. 7. A comparison like this might however be impossible in a more complicated part, where an analytical or semi-analytical solution is unlikely exist.

I recommend adaptive mesh refinement as an effective approach to improving a future model, a common technique. It uses the FE results of very coarse, simple meshes to find areas of high stress variation and make the mesh finer in those areas. After an repeating this process several times a well-tuned mesh can be made to produce the most accurate results in the least computation time.

4.0.3 Comparison Between Force and Displacement Driving Condition

When a uniform horizontal stress is applied to the end of the plate as in the other experiments, the resulting displacement distribution at the right edge of the plate is roughly linear (increasing downwards). Correspondingly, when a uniform horizontal displacement is applied to the end of the plate instead, the resulting stress distribution at the right edge of the plate is roughly linear (increasing upwards).

This demonstrates that the two scenarios are physically different in the asymmetric plate case (they would have been identical in the symmetric case). Either could be a more realistic representation of reality depending on the way the loading is applied, although for small-displacement cases like this the impact on stress concentration factors is likely to be small (this was not investigated in this report).

I noticed no difference in stability between the force and displacement-controlled analyses. In a more complex scenario perhaps this would be different - I predict displacement control in cases with large forces and displacements might have a significant stability advantage over force control.

5 Conclusion

In this case denser meshes, quadratic (over linear) shape functions, and selective element size distributions provided highest accuracy per unit of computation time, so in a practical case might be good approaches to take in designing a FE simulation. I suggested adaptive mesh refinement as a way to improve the accuracy further, by manually making the mesh finer in areas with larger stress concentrations.

Care should however always be taken to ensure results reflect reality. In this experiment, the zones with largest stress variations (and thus least accurate FE Von Mises stress predictions) - the top and bottom edges of the hole - were also the points where plastic yield would occur first. If the error of these predictions with respect to the true failure stress is not known, a real-life construction might fail unexpectedly.

References

Liu, B. and Clarkson, J. (2023). 3c7 lab report. https://www.vle.cam.ac.uk/pluginfile.php/27948449/modresource/content/1/3C7lab2023.pdf.